Environmental Science and Pollution Research (2019) 26:11998–12013
https://doi.org/10.1007/s11356-019-04652-x

RESEARCH ARTICLE

Toxic effect of different types of titanium dioxide nanoparticles on *Ceriodaphnia dubia* in a freshwater system

Velu Iswarya[1] · Abirami Palanivel[1] · Natarajan Chandrasekaran[1] · Amitava Mukherjee[1]

Received: 21 October 2018 / Accepted: 19 February 2019 / Published online: 2 March 2019

Abstract

In the current study, the effect of different types of titanium dioxide (TiO_2) nanoparticles (NPs) (rutile, anatase, and mixture) was analyzed on *Ceriodaphnia dubia* in the presence of algae under distinct irradiation conditions such as visible and UV-A. The toxicity experiments were performed in sterile freshwater to mimic the chemical composition of the freshwater system. In addition, the oxidative stress biomarkers such as MDA, catalase, and GSH were analyzed to elucidate the stress induced by the NPs on daphnids. Individually, both rutile and anatase NPs induced similar mortality under both visible and UV-A irradiations at all the test concentrations except 600 and 1200 μM where rutile induced higher mortality under UV-A. Upon visible irradiation, the binary mixture exhibited a synergistic effect at their lower concentration and an additive effect at higher concentrations. In contrast, UV-A irradiation demonstrated the additive effect of mixture except for 1200 μM which elucidated antagonistic effect. Mathematical model confirmed the effects of the binary mixture. The surface interaction between the individual NPs in the form of aggregation played a pivotal role in the induction of specific effects exhibited by the binary mixture. Oxidative stress biomarkers were highly increased upon NPs exposure especially under visible irradiation. These observations elucidated that the irradiation and crystallinity effect of TiO_2 NPs were noted only on certain biomarkers and not on the mortality.

Keywords Crystallinity · Irradiation · Mixture · Mortality · Oxidative stress markers · TiO_2 NPs

Introduction

The worldwide nanoparticles (NPs) utilization has been expected to reach 584,984 metric tons in 2019 from 225,060 metric tons (2014) with a 21.1% annual growth rate (McWilliams 2014). Among the various NPs utilized, titanium dioxide nanoparticles (TiO_2 NPs) were the highly used metal oxide NPs which received enormous importance due to their specific properties like higher photocatalytic action, as a semiconductor, and super hydrophilicity nature under UV light (Bottero and Wiesner 2010; Fan et al. 2014; Huang et al. 2010). TiO_2 NPs have been applied in various industrial sectors such as in agriculture for accelerating plant growth (Zahra et al. 2017), cosmetics and paints as a UV (ultraviolet) absorber and pigments (Mueller and Nowack 2008), the food sector as an additive and in packaging's (Yang et al. 2014), the semiconductor industry (Bai et al. 2014), medicinal sectors (Ou et al. 2016), and a few other applications like in environmental remediation (Wang et al. 2016), construction and sports materials (Harifi and Montazer 2017), and sensing (Jiang and Zhang 2009), etc. They were also commonly utilized in consumer commodities from sunscreens to electronic products (Vance et al. 2015).

As a consequence of the enormous usage, TiO_2 NPs gain access into the aquatic environment mainly through the consumer products, run-off, and wastes generated at both consumer and manufacturer levels (Gondikas et al. 2014; Gottschalk et al. 2015). Botta et al. (2011) observed a notable discharge of sub-micron-sized TiO_2 NPs from sunscreens upon aging, which constitutes of about 30% of NPs initially present in the sunscreen. From the literature reports, it has been apparent that the excessive usage of TiO_2 NPs, especially in the consumer products, was the foremost reason behind their remarkable exposure into the environment (Keller et al. 2013; Windler et al. 2012). Recently, Shandilya et al. (2015) inspected the impact of weathering (air and water) on TiO_2 NPs coatings used in building materials. A slow release of

Responsible editor: Philippe Garrigues

✉ Amitava Mukherjee
amit.mookerjea@gmail.com; amitav@vit.ac.in

[1] Centre for Nanobiotechnology, Vellore Institute of Technology, Vellore 632014, India

TiO_2 NPs into the air and water has been observed via abrasions and leaching which occurred in the coatings during the course of the period (7 months) analyzed in the study. As a result, the released NPs might interact with the organisms present in the aquatic system and may induce considerable toxic effects. Hence, it is indispensable to evaluate the impact of TiO_2 NPs on various aquatic organisms.

Daphnia species are microscopic crustaceans which are usually present in the freshwater environment. They are non-selective filter feeders, which feeds on phytoplankton and tiny particles below the size range of 50 μm (Hund-Rinke and Simon 2006; Lampert 1987). Due to its ease of availability, handling, and high sensitivity to the pollutants in the ecosystem (Tatarazako and Oda 2007), *Daphnia* sp. has been widely used as a model organism for the ecotoxicological studies and risk assessment of nanoparticles. Das et al. (2013) assessed the effect of surface capping on the toxicity of TiO_2 NPs on *Daphnia magna.* Uncapped TiO_2 NPs induced higher mortality than the carboxy-functionalized TiO_2 NPs. Several studies on TiO_2 NPs have correlated the toxicity of TiO_2 NPs with the ROS generation and indicated the importance of oxidative stress on the NPs toxicity (Clemente et al. 2014; Kim et al. 2010). Apart from the TiO_2 NPs, food available in the test matrix acts as another stressor and impacts the toxicity of NPs on daphnia. Allen et al. (2010) noticed a decrement in the silver NPs toxicity in the presence of algae. It has been suggested that the nutrition availability alters the survival efficiency of daphnids by providing the sufficient energy required for their growth and reproduction (Conine and Frost 2017). Though the TiO_2 NPs toxicity studies on aquatic organisms were carried out on different modes (Dalai et al. 2014; Wang et al. 2017), the impact of food on NPs toxicity remains ambiguous. Henceforth, the effect of fresh algae on NPs toxicity on daphnia has to be considered as it implies the environmental scenario.

As TiO_2 NPs possess distinct crystalline forms (rutile, anatase, and brookite), the toxicity profile of TiO_2 NPs concerning their crystalline forms has to be explored. Even though the crystallinity-based toxicity studies were available for TiO_2 NPs especially the anatase and P25 forms (Clemente et al. 2014; Jacobasch et al. 2014), their detailed mechanism and the other crystalline form, rutile which also has a remarkable economic application (Yu et al. 2013), were not well explored in detail. It has been well known that the variation in irradiation has a significant impact on the toxic effect of TiO_2 NPs owing to its photocatalytic differences upon irradiation (Li et al. 2016; Lu et al. 2017b). Other than these factors, aquatic components such as natural colloids and suspended matter also come into action in the aquatic system, which cannot be predicted with the present laboratory studies as they were tested mostly in the supplemented media (Hegde et al. 2016). In a study by Wormington et al. (2017), the presence of natural organic matter (NOM) inhibited the toxic effect of TiO_2 NPs to a greater extent owing to their decreased ROS (reactive oxygen species) generation but not by UV attenuation. Henceforth, it is imperative to evaluate the toxic profile of TiO_2 NPs in a similar environmental matrix with importance to their crystallinity and irradiation condition.

Owing to the wider release of distinct NPs into the aquatic environment, NPs interactions with other nanoparticles were inevitable. As a consequence, it may induce significant alterations in their toxic effects. Investigations on the toxic effects of nanoparticles as a mixture have been emerging gradually in the recent few years (Kathawala et al. 2015; Ko et al. 2017; Zou et al. 2014). Only a few studies have been evaluated on aquatic organisms regarding the toxicity of nanoparticles as a mixture (Costa 2015; Ko et al. 2018; Ye et al. 2017). Recently, Lu et al. (2017a) analyzed the mixture effects of copper (Cu) and chromium (Cr) NPs on *D. magna* in artificial freshwater and observed a distinct toxic effect when compared with their individual NPs. Co-exposure of Cu and Cr NPs resulted in similar toxicity as of Cu NPs and less toxic in comparison with Cr NPs alone. In another study, a binary mixture of zinc oxide (ZnO) and graphene oxide NPs exhibited discrete effects based on the type of organisms tested. Mixture exhibited an antagonistic effect on *Danio rerio*, and additive effect on both *Scenedesmus obliquus* and *D. magna* (Ye et al. 2018). Upon realizing the current scenario on nanoparticles buildup, it is mandatory to scrutinize the impact of NPs mixture in the freshwater system.

The current study aims to elucidate the toxic effects of TiO_2 NPs (rutile, anatase, and their mixture) on *Ceriodaphnia dubia* in the presence of algae under a similar freshwater environment, with an importance to their crystallinity. Here, the algal diet was provided to daphnids as the algal species were also available in the freshwater environment along with the NPs, which may impact the NPs toxicity. In addition, the sterile freshwater has been employed as a test medium to mimic the chemical matrix of the freshwater environment. The biochemical markers such as malondialdehyde (MDA), catalase, and reduced glutathione (GSH) were also analyzed to elucidate the oxidative stress induced by the TiO_2 NPs on *C. dubia*. These biomarkers were selected based on the mechanism of antioxidant systems and the type of end product formed in response to ROS induced by the NPs. Moreover, the influence of irradiation on TiO_2 NPs toxicity was also determined by analyzing the effect of TiO_2 NPs under two different irradiation conditions such as visible and UV-A—the two common light sources which were available to the daphnids in the natural freshwater system.

Materials and methods

Chemicals

BG-11 broth; trichloroacetic acid (TCA); 2-thiobarbituric acid (TBA); TRIS HCl; 5,5-dithiobis-[2-nitrobenzoic acid]

(DTNB); and malondialdehyde (MDA) were purchased from Hi-media Laboratories Pvt. Ltd., Mumbai, India. Reduced glutathione (GSH) was procured from the manufacturer, Sigma-Aldrich, MO, USA. Hydrogen peroxide (30% *w/v* H_2O_2) was obtained from Sd fine-chem limited, Mumbai, India. All the other reagents utilized in the study were of analytical grade.

Nanoparticles and their preparation

Distinct TiO_2 NPs varying in their crystalline phases such as anatase (CAS No: 1317-70-0) and rutile (CAS No: 1317-80-2) NPs were obtained from the manufacturer, Sigma-Aldrich, USA. The particle sizes of the anatase and rutile NPs were advertized as < 25 nm and < 100 nm (~ 10 nm diam. × 40 nm L), respectively. NPs suspension with the stock concentration of about 5 mM was prepared in the de-ionized water and utilized for the toxicity assays. Further, they were sonicated at 20 kHz frequency for about 20 min with the help of a 130-W ultrasonicator (Sonics, USA) to achieve a homogenous suspension of TiO_2 nanoparticles. Both the TiO_2 NPs were characterized by various techniques (electron microscopy, dynamic light scattering (DLS)) and reported in our previous studies (Iswarya et al. 2015). NPs suspension characterized by transmission electron microscopy (TEM, Fig. 1) disclosed that the primary sizes of the TiO_2 NPs were noted to be 32.63 ± 2.73 nm in length and 5.97 ± 0.49 nm in breadth for rutile NPs, and 11 ± 0.54 nm for anatase NPs. It was also remarked that the rutile NPs were rod-shaped, and the anatase NPs were spherical. Henceforth, the size analysis through the TEM and DLS disclosed that the sizes of rutile and anatase NPs were almost similar. Thus, the abovementioned NPs were further utilized for the assessment of the crystalline effect of TiO_2 NPs.

Experimental matrix and test species

Sterile freshwater prepared from the freshwater obtained from the VIT Lake was utilized as an experimental matrix for the entire experiment carried out in the present study. The collected freshwater was initially filtered with the series of filters such as blotting paper and Whatman no. 1 and followed by its sterilization to be devoid of debris and microbes present in it. The sterilization process was attained by autoclaving the filtered freshwater at 121 °C, 15 psi for about 15 min such that the chemical composition of the freshwater remains intact. This filter-sterilized freshwater was further expressed as sterile freshwater throughout the study. Thus, the freshwater system has been mimicked by the utilization of sterile freshwater as an experimental matrix in this study. The physicochemical parameters of the sterile freshwater have been characterized and detailed in our previous study (Iswarya et al. 2018).

Freshwater daphnia, *C. dubia*, was used as a test species for evaluating the toxicity assessment of TiO_2 NPs. *Chlorella* sp., a freshwater alga, has been provided as a feed for *C. dubia*. Both the organisms were isolated from the VIT Lake located in the Vellore Institute of Technology, Vellore, India, and maintained in our laboratory under specified conditions (visible light, day/night rhythm of 16 h/8 h, 24 °C). Experimental procedures regarding the isolation of freshwater organisms were reported briefly in our previous studies (Iswarya et al. 2015; Iswarya et al. 2016a). White fluorescent lights (Philips Life Max, 18 W with an intensity of 1.8 W/m^2) have been utilized to provide the visible light for the test organisms to maintain the day and night rhythm. Sterile freshwater was used as a sub-culture media for the maintenance of *C. dubia*, while the BG-11 medium was used for the subsistence of *Chlorella* sp.

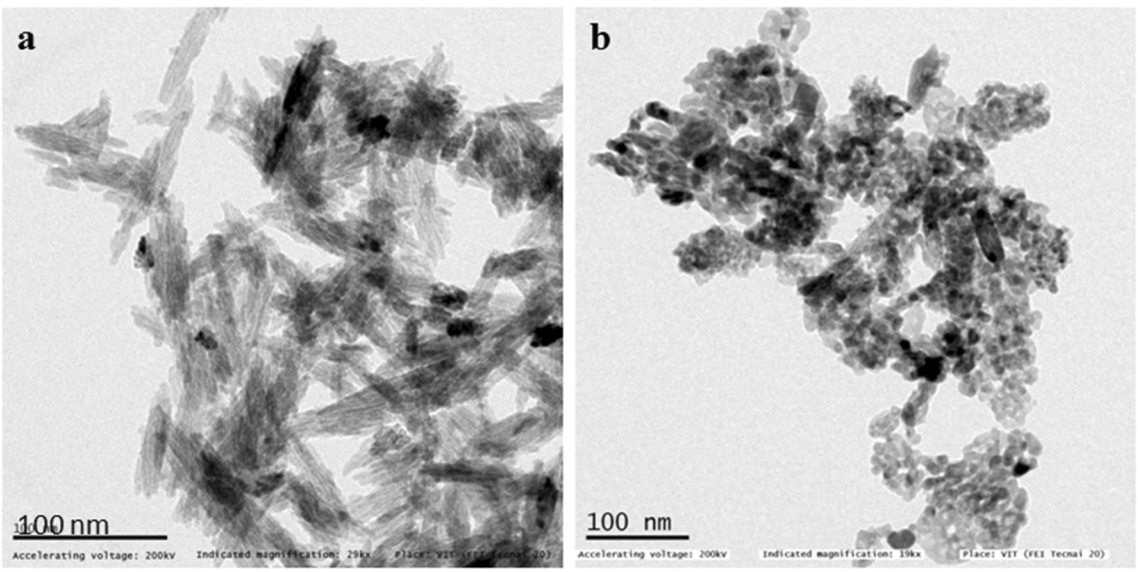

Fig. 1 TEM images of the **a** rutile NPs, and **b** anatase NPs

Experimental design

Algal cells devoid of sub-culture media were harvested from the 28-day old stock cultures of *Chlorella* sp. by means of centrifugation at 7000 rpm at 4 °C for about 10 min. From the algal cells harvested, an optical density (OD) of 0.1 OD which consists 1×10^5 cells was prepared in the sterile freshwater. To the exposure medium, i.e., the sterile freshwater comprising 0.1 OD of algal cells, TiO_2 NPs (rutile, anatase, and mixture) and 24-h-old neonates were added. The number of daphnids added to the exposure medium was varied based on the assay performed, viz., ten for mortality and 30 for oxidative stress assessments. As per the OECD guideline of 2 mL of the exposure medium per daphnid (OECD 2004), about 20 and 60 mL of the exposure medium was maintained for mortality and oxidative stress experiments, accordingly. Various concentrations of TiO_2 NPs in an array of 75–1200 μM were selected for the toxicity assays. Whereas the rutile and anatase NPs were taken in the equivalent ratio for the binary mixture, i.e., the binary mixture comprises an equal concentration of rutile and anatase NPs. For instance, 300 μM of binary mixture consists of 150 μM of rutile NPs and 150 μM of anatase NPs such that the total concentration of the mixture is 300 μM. After the addition of neonates, they were kept under visible and UV-A irradiations for about 48 h under photoperiodic conditions, i.e., 16 h light and 8 h dark. A similar experiment has been followed for the negative control, i.e., in the absence of TiO_2 NPs, which has been further portrayed as untreated daphnids (0 μM). Moreover, separate control groups were maintained for visible and UV-A irradiation. White fluorescent tubes (1.8 W/m^2 intensity, Philips) and black tubes (2.3 W/m^2 intensity, Philips) were utilized to afford visible and UV-A light for the daphnids, respectively. After the 48-h exposure to TiO_2 NPs, the mortality assessment and the oxidative stress assays were performed.

Mortality assessment

Various concentrations of TiO_2 NPs such as 0, 75, 150, 300, 600, and 1200 μM were selected for the mortality studies on *C. dubia*. About ten neonates were utilized to assess the mortality of *C. dubia* upon exposure to TiO_2 NPs. After the 48-h exposure to TiO_2 NPs, the number of neonates alive was counted and the data were expressed in terms of mortality percentage after its normalization with the untreated daphnids. From the mortality data, a mathematical model described by Abbott (1925) and Chesworth et al. (2004) has been executed to determine the type of interaction induced by the rutile and anatase NPs when they were co-exposed together. Expected mortality has been computed from the percentage mortality obtained for the individual NPs such as rutile (R) and anatase (A) NPs with the help of Eq. 1:

$$\text{Expected mortality} = R + A - (R \times A/100) \quad (1)$$

where, R and A indicates the percentage mortality observed for rutile and anatase NPs individually, respectively. Further, the ratio of inhibition was computed using Eq. 2 by comparing the observed mortality with their expected mortality:

$$\text{Ratio of Inhibition } (R_I) = \text{Observed mortality}/\text{Expected mortality} \quad (2)$$

Based on the R_I values obtained, the effect of the mixture has been categorized into synergistic ($R_I > 1$), additive ($R_I = 1$), and antagonistic ($R_I < 1$). The obtained effects were considered as an additive if the R_I values were not statistically varied from 1. In addition, the differences noted among the observed and expected mortality were statistically validated with the help of two-way ANOVA (Tukey multiple comparison tests) at the p value less than 0.05.

Aggregation profile of TiO_2 NPs in the sterile freshwater

The aggregation profile of TiO_2 NPs such as rutile, anatase, and binary mixture has been assessed in the sterile freshwater to determine the colloidal stability of TiO_2 nanoparticles in the freshwater system. The aggregation profile of NPs was analyzed only at the specific concentrations of TiO_2 NPs such as 75, 300, and 1200 μM under both visible and UV-A irradiations. The effective diameter of TiO_2 NPs (rutile, anatase, and mixture) was determined using a Nanobrook particle size analyzer (90 Plus PALS, Brookhaven Instrument, USA) at distinct time intervals like 0 and 2 h. The abovementioned analysis was terminated after 2 h due to the micron size of NPs which cannot be measured with the particle size analyzer whose sensitivity was limited to 10 μm.

Additionally, the surface interactions between rutile and anatase NPs when they coexist as a binary mixture have been analyzed using transmission electron microscopy (TEM). Higher concentration of the binary mixture (1200 μM) was prepared in the sterile freshwater and subjected to irradiation under both visible and UV-A conditions for about 48 h. An aliquot of the suspension was placed on the copper grids and observed under high-resolution TEM (FEI Technai G2 T20 S-Twin, USA).

Oxidative stress markers

The oxidative stress induced by the TiO_2 NPs has been further assessed on the daphnids treated with TiO_2 NPs at the selected concentrations (0, 75, 300, and 1200 μM) with the help of

certain biomarkers such as MDA, catalase, and GSH, etc. For oxidative stress analysis, about 30 daphnids (< 24 h) were exposed to TiO_2 NPs for about 48 h under distinct irradiations—visible and UV-A. Control daphnids were also kept in parallel without any exposure to NPs under a similar experimental condition for both visible and UV-A irradiations. After 48-h exposure, the live daphnids (NPs-treated and untreated) were collected from the experimental medium and utilized for further assessments. Moreover, about 30 daphnids were maintained per sample from the replicates kept for the study such that the mass of the daphnids was quite enough to perform the assays. In case of insufficient daphnids, daphnids were collected from other replicates and maintained as individual samples such that their biomass was kept unique. The collected daphnids were washed in de-ionized water to eliminate the loosely bound TiO_2 NPs if any. Then, the daphnids were homogenized in 1 mL of potassium phosphate buffer (0.1 M with pH 7.4) by means of an ultrasonicator (130 W, Sonics, USA) for 2 min and centrifuged at 10,000 rpm for 15 min at 4 °C. The whole homogenization process was performed on ice to avoid the generation of artifacts (ROS) during the course of ultrasonication. The pellet obtained after the process of centrifugation was utilized for MDA assay, while the supernatant was utilized for other assays. After the biomarker analysis, the obtained values were computed for individual daphnid by normalizing the biomarker data with the total number of daphnids utilized for the assay.

MDA assay

A renowned lipid peroxidation biomarker, malondialdehyde (MDA), was estimated to determine the oxidative stress induced by the nanoparticles on the daphnids. MDA assay has been performed as per the protocol described by Buege and Aust (1978). To the pellet obtained, 1 mL of 1 M TRIS HCl with the pH of 7.4 was added, well mixed and incubated at 37 °C for 30 min. Then, 2 mL of TCA-TBA reagent (0.375% TBA in 5%TCA) was added and vortexed for a while. The reaction mixture was then kept in a hot water bath at 90 °C for about 45 min. After a few minutes of cooling, the solution obtained was centrifuged at 4 °C for about 10 min at the speed of 3000 rpm. The absorbance of the supernatant obtained after the centrifugation step was measured at 535 nm using a UV-visible spectrophotometer (U2910, Hitachi, Japan). The amount of MDA produced in the sample was computed with the MDA standard curve and expressed in the unit of picomolar/daphnid after its normalization with the total number of daphnids utilized for the assay.

Catalase assay

Catalase assay has been performed according to the standard procedure prescribed by Aebi (1974). The reaction mixture comprising of 30 μL of the supernatant, 670 μL of potassium phosphate buffer (50 mM, pH 6.6), and 330 μl of 30 mM H_2O_2 prepared in potassium phosphate buffer was measured at 240 nm for about 3 min with the help of the UV-visible spectrophotometer. The rate of decrease in the absorbance was computed, and their enzyme activity was calculated in terms of milliunit/milliliter using its molar extinction coefficient, 0.0436 mM^{-1} cm^{-1}. Then, the results were expressed in the unit of milliunit/milliliter/daphnid after its normalization with the total number of daphnids utilized for the assessment.

GSH assay

Reduced glutathione (GSH) assay has been performed as per the protocol described by Sedlak and Lindsay (1968) with slight modifications. Initially, the solution comprising 62.5 μL supernatant and 400 μL distilled water was precipitated with 5% TCA (12.5 μL). Then, the precipitated solution was centrifuged at 4 °C for 10 min at 6000 rpm. The supernatant obtained after the centrifugation step was utilized for GSH analysis. The mixture containing 50 μL of the supernatant, 200 μL of potassium phosphate buffer (0.2 M, pH 8.0), and 10 μL of DTNB (0.6 mM in 0.2 M potassium phosphate buffer, pH 8.0) were added to the 96-well plate, and their absorbance was read at 412 nm with the help of a microplate spectrophotometer (Powerwave XS2, Biotek). Further, the total amount of GSH produced by the daphnids was computed with the help of the curve obtained from the standard, reduced glutathione, and the results were expressed in the unit of picomolar/daphnid after its normalization with the total number of daphnids.

Statistical analysis

All the analyses were carried out in triplicates at least in three groups from the same batch of daphnids, and the results were represented in mean ± standard error. Analysis of variance (ANOVA) was executed with the help of the statistical software, GraphPad Prism, version 6.01. The statistical difference between the NPs-treated and NPs-untreated daphnids was evaluated with the help of two-way ANOVA (Tukey multiple comparison tests, $p < 0.05$). Furthermore, the variations among the different types of TiO_2 NPs such as anatase, rutile, and mixture were also tested with two-way ANOVA at the level of significance, $p < 0.05$. In the same way, the significant variations between the visible and UV-A irradiations were also analyzed.

Results

Mortality assessment

Mortality induced by the distinct types of TiO_2 NPs such as rutile, anatase, and mixture has been represented in Fig. 2.

Under both visible and UV-A irradiations, a concentration-dependent incline in the mortality was noticed for the TiO_2 NPs irrespective of its types such as rutile, anatase, and mixture. The daphnids exposed to 1200 μM of rutile, anatase, and mixture exhibited a mortality percentage of about 26 ± 2.45, 24 ± 2.45, and 30 ± 0% under visible irradiation. Mortality produced by the TiO_2 NPs under visible irradiation was statistically different ($p < 0.05$) from their untreated daphnids at all the test concentrations employed in the study, except at 75 and 150 μM of individual NPs, while the daphnids exhibited 46 ± 2.45, 30 ± 4.47, and 28 ± 2% mortality under UV-A irradiation upon exposure to 1200 μM of rutile, anatase, and mixture, respectively. Similar to the visible irradiation, the mortality observed under UV-A irradiation was significantly different ($p < 0.05$) from the untreated daphnids at all the concentrations of TiO_2 NPs analyzed in the study, except at 75 μM of all the types of TiO_2 NPs and 150–300 μM of rutile NPs.

Individually, anatase and rutile NPs did not exhibit any significant difference in the mortality ($p > 0.05$) at all the concentrations tested under both the irradiation conditions, except 600 and 1200 μM at UV-A irradiation. Juxtaposing the individual NPs with the mixture, binary mixture showed the highest mortality than individual NPs under visible irradiation. The differences observed among the mortality of individual NPs and mixture were statistically significant ($p < 0.05$) at all the concentrations tested except at 1200 μM under visible irradiation. Like visible irradiation, binary mixture exhibited higher mortality than that of rutile NPs under UV-A irradiation at all the concentrations tested, excluding 600 and 1200 μM. The differences observed among the mortality of rutile NPs and mixture were statistically significant ($p < 0.05$) at all the test concentrations except at 75 μM under UV-A irradiation, while the anatase NPs did not show any significant difference ($p > 0.05$) in their mortality upon its comparison with the mixture under UV-A irradiation. Moreover, the differences observed between the mortality of visible and UV-A irradiations were statistically insignificant ($p > 0.05$) irrespective of the types of TiO_2 NPs such as rutile, anatase, and mixture at all the concentrations tested, except at 600 and 1200 μM of rutile NPs.

Mathematical modeling of the mixture

A mathematical model has been utilized to characterize the mode of action that persists when the rutile and anatase NPs coexist as a mixture. R_I values computed for the mixture has been represented in Table 1. Due to the discrepancy in the mortality values like zero mortality, R_I values were not computed for certain concentrations of the mixture such as 75 and 150 μM under visible irradiation and 75 μM under UV-A irradiation. The highest R_I value of about 2.29 ± 0.21 was observed at 300 μM of mixture, indicating its synergistic effect under visible irradiation. Whereas, the lowest R_I value of about 0.61 ± 0.04 was noted at 1200 μM under UV-A irradiation representing the antagonistic action of mixture since its R_I value was less than 1. On the contrary, an additive effect was noted at the concentration of 150–600 μM under UV-A irradiation and 600–1200 μM under visible irradiation with the R_I value of 1. As the concentration of mixture increases, the R_I value of the mixture was found to be decreased under both visible and UV-A irradiation. It signifies that the action of rutile and anatase NPs were decreased when they coexist as a mixture, particularly at their higher concentrations.

Aggregation profile of TiO_2 NPs in sterile freshwater

The aggregation profile of 75, 300, and 1200 μM TiO_2 NPs (rutile, anatase, and mixture) in the sterile freshwater was analyzed at various time intervals such as 0 and 2 h using DLS and has been represented in Fig. 3. TiO_2 NPs irrespective of their types showed an increase in their effective diameter as the time progressed. Initially at 0 h, the effective diameter of 1200 μM TiO_2 NPs in the sterile freshwater was noted to be 988.75 ± 43.38, 732 ± 17.98, and 754.94 ± 7.19 nm for rutile, anatase, and binary mixture, respectively. Their initial sizes were gradually increased to 6945.01 ± 455.06 nm (rutile NPs), 3510.29 ± 31.87 nm, (anatase NPs), and 4617.25 ± 139.43 nm (mixture) after 2 h irradiation with visible light. Similarly, UV-A irradiation also enhanced their initial sizes into 7231.09 ± 270.83, 3481.44 ± 227.22, and 5338 ± 254.01 nm for rutile, anatase, and mixture, respectively. The difference in the sizes of TiO_2 NPs (all the forms) noted between 0 and 2 h was statistically significant ($p < 0.05$) under both visible and UV-A irradiations tested in the study. Contrasting the visible and UV-A irradiation, all the types of TiO_2 NPs such as anatase, rutile, and mixture showed a significantly higher aggregation ($p < 0.05$) under UV-A irradiation with respect to their concentrations studied, except 300 μM of anatase NPs and 1200 μM of TiO_2 NPs irrespective of their forms. Individually, anatase NPs were noted to be quite stable than the rutile NPs. These differences were significant at all the concentrations for both visible and UV-A irradiations ($p < 0.05$). Comparing the rutile NPs with the binary mixture, the size of the rutile NPs was found to be statistically high ($p < 0.05$) than the size of the mixture under both irradiations at all the concentrations employed. In contrast, anatase NPs showed lesser aggregation in the sterile freshwater than the binary mixture at all the concentrations and irradiations tested in the study. The differences in their sizes were statistically different ($p < 0.05$).

The surface interaction between rutile and anatase NPs when coexisting as a mixture in the sterile freshwater has been illustrated with the help of transmission electron microscopy. TEM images of the binary mixture after visible and UV-A irradiations were represented in Figs. 4 and 5, respectively. Similar surface interactions were noticed under both visible

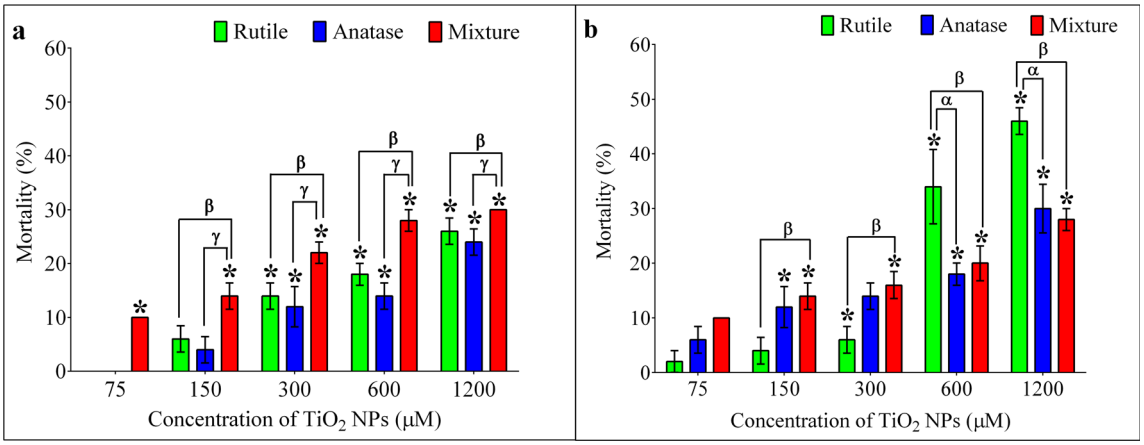

Fig. 2 Mortality induced by the various types of TiO_2 NPs (rutile, anatase, and mixture) under different irradiation conditions such as **a** visible and **b** UV-A irradiation on *C. dubia*. The asterisk (*) symbol represents that the mortality (%) observed for the TiO_2 NPs was statistically significant ($p < 0.05$) from the untreated daphnids. Similarly, the alpha (α) and beta (β) symbol depicts that the mortality obtained for the rutile NPs was statistically different from the mortality observed for anatase NPs and mixture, respectively, while the "γ" symbol indicates that the mortality differences observed between the anatase NPs and the mixture were significant

and UV-A irradiations. The binary mixture showed a complex and rapid aggregation of NPs in the sterile freshwater (Figs. 4a and 5a) as similar to DLS data. It was also noticed that the anatase NPs were encompassed by the rutile NPs (Figs. 4c and 5c) owing to their interparticle interactions. Energy dispersive X-ray (EDAX) analysis confirmed the availability of dissolved carbon and inorganic ions such as Ca^{2+}, SO_4^{2+}, Cl^-, Na^+, and Mg^{2+} along with the binary mixture under both visible (Fig. 4d) and UV-A (Fig. 5d) irradiations. These ions were commonly referred as the natural colloids of the freshwater that would have played a prominent role in the surface interaction between the anatase and rutile NPs when co-exposed together as a mixture.

Oxidative stress markers

Several oxidative stress biomarkers such as MDA, catalase, and GSH were estimated to determine the changes induced on the daphnids upon interaction with the TiO_2 nanoparticles.

MDA assay

MDA assay has been performed to describe the level of lipid peroxidation on the cellular membranes of daphnids. MDA produced by the daphnids upon exposure to visible and UV-A irradiations was represented in Figs. 6a and 7a, respectively. TiO_2 NPs-treated daphnids showed the higher amount of MDA than that of untreated daphnids under both the irradiation conditions. Daphnids treated with 1200 μM of rutile, anatase, and mixture depicted MDA levels of about 3.89 ± 0.41, 3.08 ± 0.08, and 0.97 ± 0.24 pM/daphnid under visible irradiation, and 3.40 ± 0.08, 2.19 ± 0.16, and 4.21 ± 0.08 pM/daphnid under UV-A irradiation, respectively. Under visible irradiation, the amount of MDA produced by the daphnids was noted to be significantly increased ($p < 0.05$) till 300 μM, which experienced a decline at 1200 μM in case of individual NPs. In contrast, a decline in the MDA level was observed for the binary mixture with an incline in the concentration of mixture. The changes noted in the MDA of NPs-

Table 1 Mathematical model inferring the mode of action of TiO_2 NPs when rutile and anatase NPs coexist together as a mixture

Concentration of TiO_2 NPs (μM)	Expected mortality (%)	Observed mortality (%)	Statistical significance at $p < 0.05$	R_I value	Mode of action
A) Visible irradiation					
300	9.6 ± 4.25	22 ± 2	Yes	2.29 ± 0.21	Synergistic
600	24 ± 5.17	28 ± 2	No	1.17 ± 0.08	Additive
1200	29.4 ± 3.16	30 ± 0	No	1.02 ± 0	Additive
B) UV-A irradiation					
150	7.8 ± 3.58	14 ± 2.45	No	1.80 ± 0.31	Additive
300	15.2 ± 5.54	16 ± 2.45	No	1.05 ± 0.16	Additive
600	19 ± 4.02	20 ± 3.16	No	1.05 ± 0.17	Additive
1200	45.6 ± 6.4	28 ± 2	Yes	0.61 ± 0.04	Antagonistic

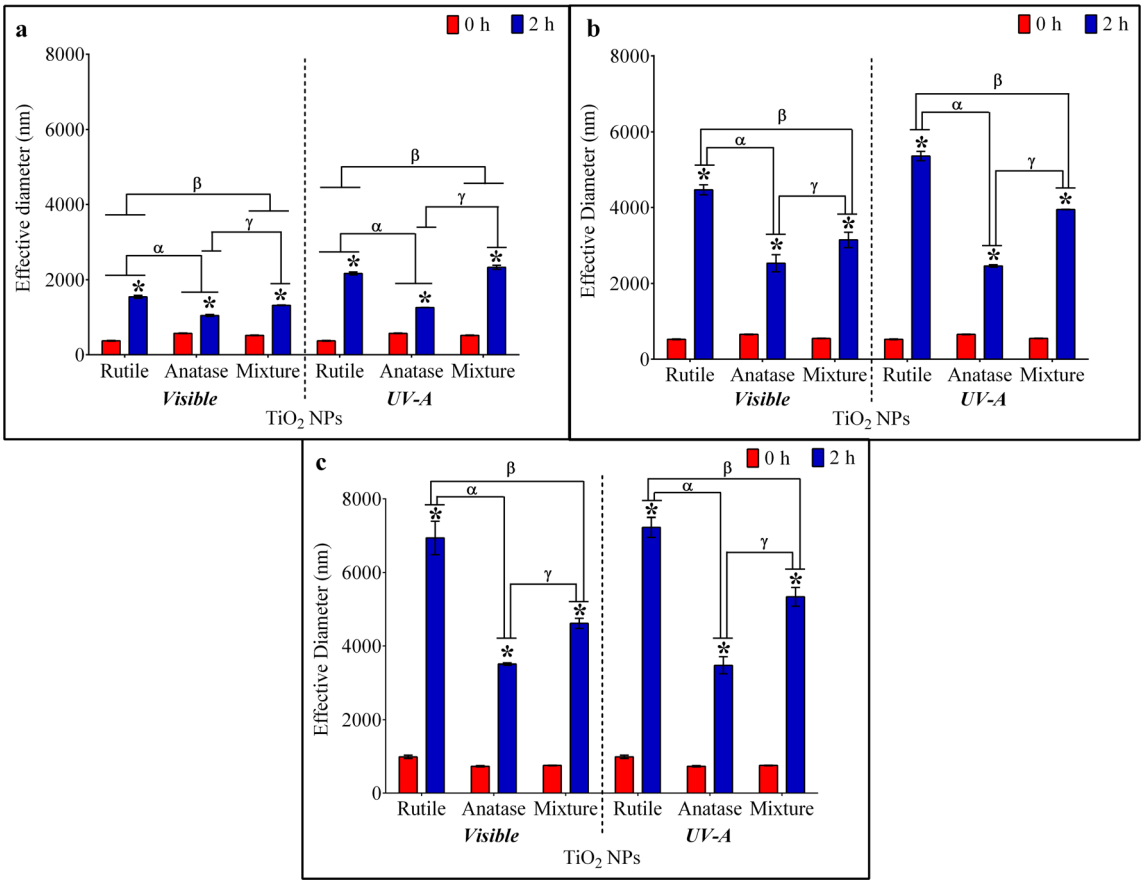

Fig. 3 Aggregation profile of different forms of TiO_2 NPs such as rutile, anatase, and mixture under visible and UV-A irradiation at various exposure concentrations such as **a** 75 μM, **b** 300 μM, and **c** 1200 μM. The symbol * depicts that the size differences noted between 0 and 2 h were statistically significant at $p < 0.05$, while the alpha (α) and beta (β) symbols signify that the sizes observed for rutile NPs were statistically different from the sizes observed for anatase NPs and mixture, respectively. Similarly, the "γ" symbol represents that the size variations observed between the anatase NPs and mixture were significant

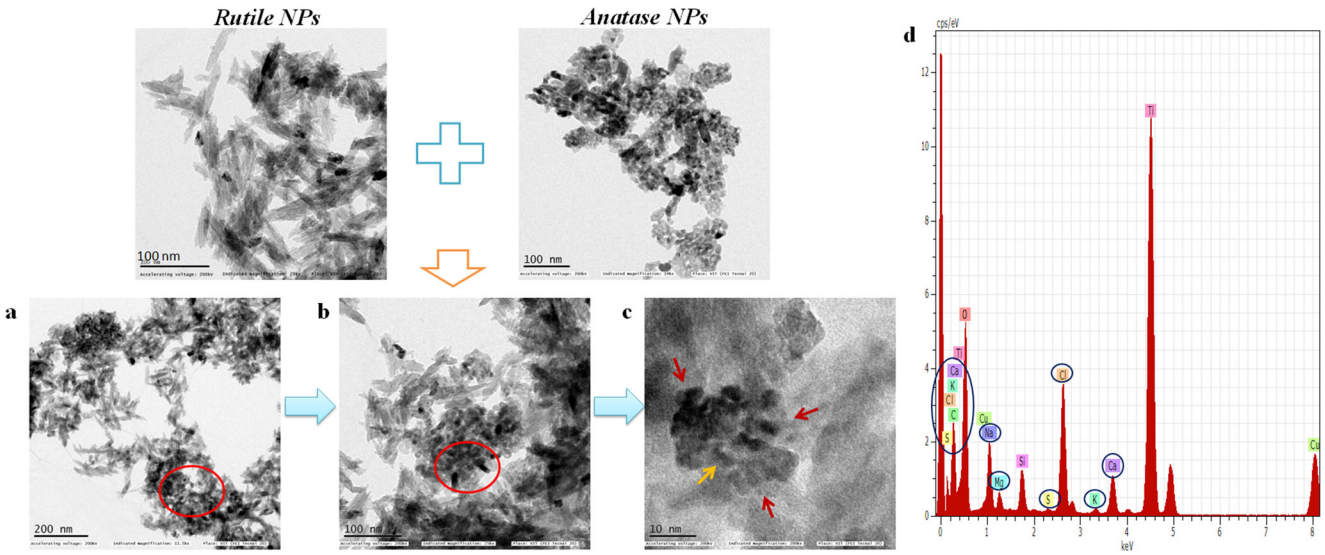

Fig. 4 TEM images of the binary mixture depicting the rutile-anatase interactions under visible irradiation after 48 h. **a** Notable aggregation of NPs upon interaction between the rutile and anatase NPs when they coexist as a mixture in the sterile freshwater. **b** Anatase NPs (spherical shaped) were covered by the rutile (rod-shaped) NPs. **c** High-resolution image of binary mixture depicting the clear confinement of anatase NPs by the rutile NPs. Yellow arrows—anatase NPs; red arrows—rutile NPs. **d** EDAX image of the binary mixture confirming the presence of inorganic ions (blue-colored ovals) and their role in the surface interactions between anatase and rutile NPs

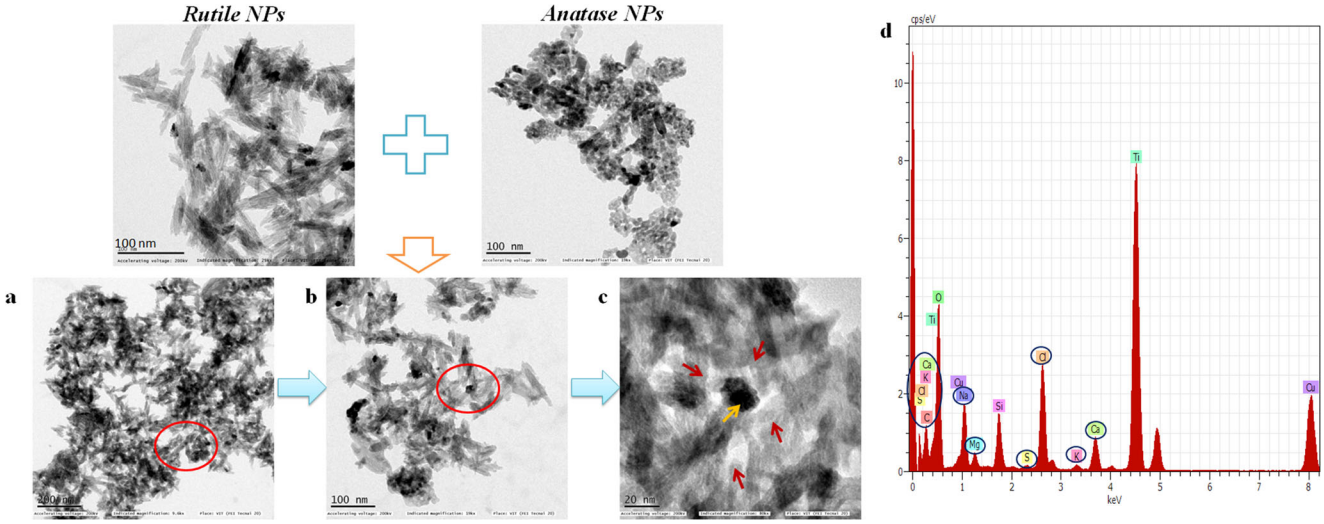

Fig. 5 TEM images of the binary mixture depicting the rutile-anatase interactions under UV-A irradiation after 48 h. **a** Substantial aggregation of NPs upon interaction between the rutile and anatase NPs when they coexist as a mixture in the sterile freshwater. **b** Anatase NPs (spherical-shaped) were enclosed by the rutile (rod-shaped) NPs. **c** High-resolution image depicting the clear confinement of rutile NPs over the anatase NPs. **d** EDAX data of the binary mixture confirmed the existence of inorganic ions (blue-colored ovals) and their role in the surface interactions between anatase and rutile NPs. Yellow arrows—anatase NPs; red arrows—rutile NPs

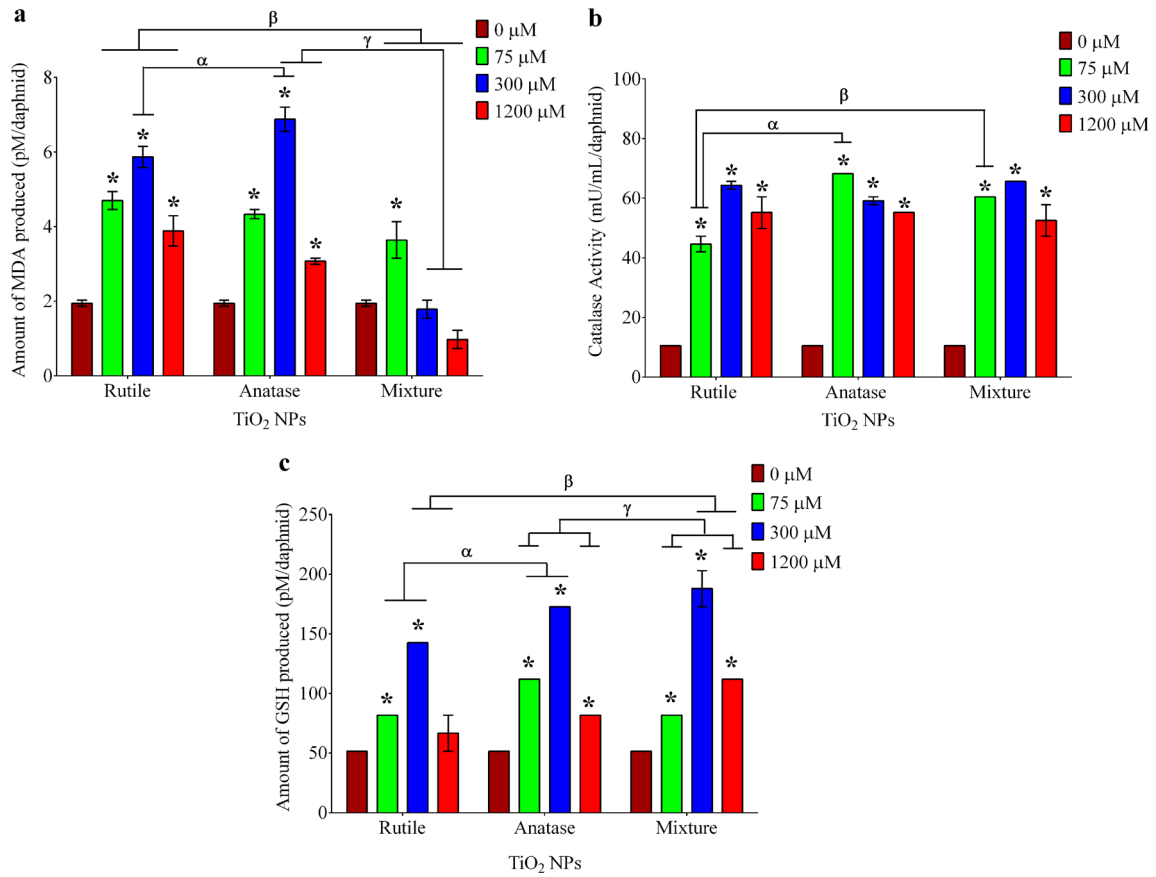

Fig. 6 Oxidative stress biomarkers assessed on the daphnids after its treatment with various types of TiO_2 NPs such as rutile, anatase, and mixture under visible irradiation. **a** MDA, **b** catalase, and **c** GSH. The symbol "*" indicates that the levels of markers generated by the TiO_2-treated daphnids were statistically significant with respect to their respective markers induced on the untreated daphnids. The symbol "α" depicts that the differences noted between the rutile and anatase NPs were statistically significant. Similarly, the symbol "β" represents the significant differences noted among the rutile NPs and mixture, and the "γ" symbol indicates the significant differences between the anatase NPs and mixture

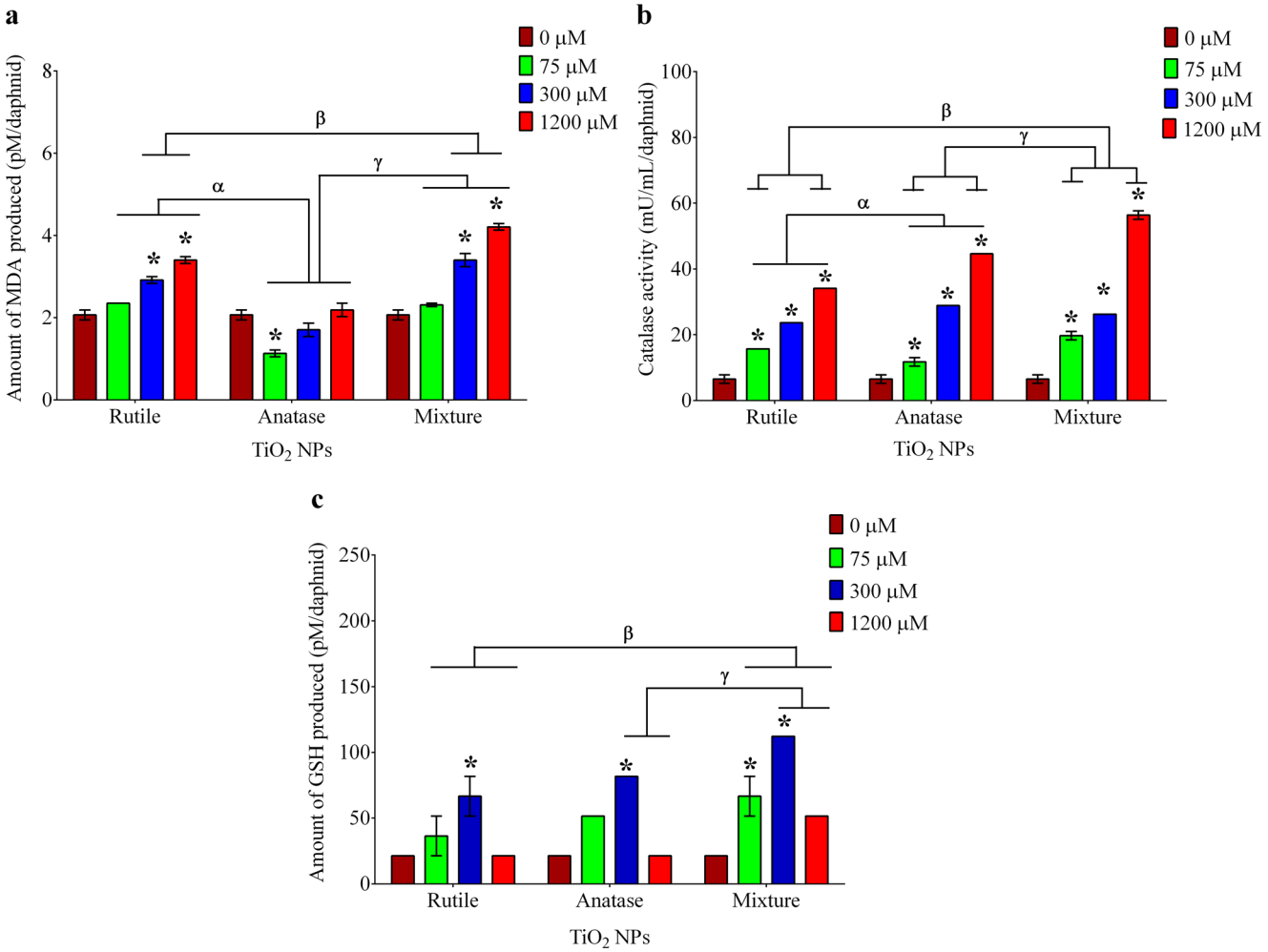

Fig. 7 Oxidative stress biomarkers assessed on the daphnids treated with TiO_2 NPs (rutile, anatase, and mixture) under UV-A irradiation. **a** MDA, **b** catalase, and **c** GSH. The asterisk symbol (*) represents that the markers produced by the TiO_2-treated daphnids were significantly different from the markers of untreated daphnids. The alpha symbol (α) indicates that the variations observed between the rutile and anatase NPs were statistically different, while the significant differences noted between the rutile NPs and the mixture were represented by the "β" symbol and the differences between the anatase NPs and the mixture were indicated by the "γ" symbol

treated daphnids were statistically different ($p < 0.05$) from the MDA of untreated daphnids at all the concentrations, except at 300 and 1200 μM of the mixture. In contrast to visible irradiation, the MDA level of TiO_2 NPs-treated daphnids was increased with respect to its concentration under UV-A irradiation. In case of anatase-treated daphnids under UV-A irradiation, the amount of MDA produced by the daphnids was lesser than the MDA of untreated daphnids. This effect was not observed for the concentration of 1200 μM.

Comparing the MDA levels of visible and UV-A irradiations, MDA levels were high under visible irradiation irrespective of its phases, except the mixture which produced MDA in higher amounts at the concentrations of 300 and 1200 μM under UV-A. Among the MDA levels of individual NPs, rutile-treated daphnids showed higher MDA production than anatase-treated daphnids under both visible (except 300 μM) and UV-A irradiations. Contradicting the individual NPs with the mixture, binary mixture induced higher amounts of MDA production under UV-A irradiation. In contrast, the amount of MDA induced by the mixture was lower under visible irradiation.

Catalase assay

Catalase activity of the daphnids treated with TiO_2 NPs was evaluated and represented in Figs. 6b and 7b for visible and UV-A irradiations, respectively. Under both the irradiation conditions, catalase activity was noted to be significantly increased ($p < 0.05$) for NPs-treated daphnids as compared to their catalase activity of untreated daphnids. Upon visible irradiation, highest catalase activities of about 64.31 ± 1.31, 68.25 ± 0, and 65.62 ± 0 mU/mL/daphnid were observed for rutile (300 μM)-, anatase (75 μM)-, and mixture (300 μM)-treated daphnids, respectively. A concentration-dependent

incline in the catalase activity was observed for rutile- and mixture-treated daphnids till 300 μM under visible irradiation. In contrast, the anatase-treated daphnids showed a significant decline in the catalase activity upon an incline in the concentration of NPs under visible irradiation. In the case of UV-A irradiation, catalase activity was higher at the concentration of 1200 μM which was noted to be 34.12 ± 0, 44.62 ± 0, and 56.44 ± 1.31 mU/mL/daphnid for rutile-, anatase-, and mixture-treated daphnids. As the concentration of NPs increased, the enzyme activity of catalase was also increased significantly ($p < 0.05$) under UV-A irradiation.

Within the individual TiO_2 NPs, anatase NPs induced higher catalase activity on *C. dubia* than that of rutile NPs under UV-A irradiation. A similar effect has been noticed under visible irradiation only at the concentration of 75 μM. The differences noted in the catalase activity of individual NPs were significant at the p value < 0.05. Juxtaposing the enzyme activity of the mixture with the individual NPs, mixture-treated daphnids depicted higher catalase activity under UV-A irradiation and were significant ($p < 0.05$) at the concentrations of 75 and 1200 μM. In case of visible irradiation, the catalase action did not vary significantly ($p > 0.05$) with respect to their individual NPs. Only at the lower concentration (75 μM), the catalase action of mixture-treated daphnids was noted to be significantly ($p < 0.05$) high when compared with the rutile NPs-treated daphnids and lower with the anatase NPs-treated daphnids. Among the two irradiations tested in the study, catalase activity was significantly high ($p < 0.05$) under visible irradiation at all the concentrations employed, except 1200 μM.

GSH assay

Reduced glutathione was considered as a vital biomarker which has been commonly utilized to determine the defense capacity of the organism against the oxidative stress. The level of reduced glutathione on NPs-treated daphnids was analyzed, and the data were represented in Fig. 6c for visible irradiation and Fig. 7c for UV-A irradiation. An incline in the GSH levels was noted for NPs-treated daphnids than that of untreated daphnids under both visible and UV-A irradiations. Though an incline in the GSH levels was noted, a concentration-dependent effect has not been observed for NPs-treated daphnids under both visible and UV-A irradiations. The level of GSH was noted to be high at 300 μM under both visible and UV irradiations employed. It has been noted to be about 142.42 ± 0, 172.73 ± 0, and 187.88 ± 15.15 pM/daphnid under visible irradiation and 66.67 ± 15.15, 81.81 ± 0, and 112.12 ± 0 pM/daphnid under UV-A irradiation for rutile-, anatase-, and mixture-treated daphnids, respectively.

Among the individual NPs, GSH levels were higher for anatase-treated daphnids upon visible irradiation. These differences were significant ($p < 0.05$) at all concentrations, excluding 1200 μM. In contrast, UV-A irradiation did not induce any significant difference ($p > 0.05$) in the GSH levels upon treatment with the individual NPs. Comparing the individual NPs with the mixture, mixture-treated daphnids showed higher GSH levels than the individual NPs-treated daphnids under both the irradiation conditions, except at 75 μM of anatase NPs under visible irradiation. Contradicting the visible irradiation with UV-A, the reduced glutathione was significantly produced in higher quantity under visible irradiation irrespective of their types at all the test concentrations, except at 75 μM of the mixture.

Discussion

Toxicity of TiO_2 NPs on *C. dubia*

In the present study, the toxic effect of TiO_2 NPs (rutile, anatase, and mixture) on *C. dubia* was explored in the presence of algae under distinct irradiation conditions such as visible and UV-A irradiations in the milieu of a freshwater environment. As the concentration of TiO_2 NPs increased, toxicity was also noted to be increased (Fig. 2). Variation in the crystallinity and irradiation did not induce any effect on the mortality of TiO_2 NPs, except at the higher concentration of rutile NPs under UV-A. These results were in contrary with the earlier reports (Lu et al. 2017b) which state that the differences in the crystallinity and irradiation impact the TiO_2 NPs toxicity. Since they were mostly performed in the absence of algae, it has been apparent that the differences noted in the toxicity were chiefly due to the algal diet. Upon comparison with our previous toxicity data on TiO_2 NPs, it has been revealed that the TiO_2 NPs toxicity obtained in the presence of algae was lower than the toxicity obtained through both water-borne (Iswarya et al. 2016a) as well as a dietary exposure (Iswarya et al. 2018). A similar effect has been observed by Allen et al. (2010) and Conine and Frost (2017) while examining the toxic effects of silver nanoparticles on *D. magna*. They also discussed that algal availability mitigates the toxic effects of nanoparticles due to the alteration in the nutrition available to the daphnids. In other words, it can be presumed that the toxic effect of individual NPs was diminished when afforded with the nutrition-rich sources like algae. Besides, the EPS (exopolymeric substances) secretion by the algal cells and the surface interaction between TiO_2 NPs and algae might have enhanced the NPs aggregation and reduced the bioavailability of TiO_2 NPs in the test matrix, as stated by Sendra et al. (2017) and Dalai et al. (2013). Consequently, the TiO_2 NPs available for the ingestion by the daphnids becomes less and in turn, diminished the NPs toxicity.

From the mortality data, it was observed that the action of the binary mixture was dependent on both concentration as well as the type of irradiation exposed. The effect of the

mixture was decreased, as the concentration of TiO_2 NPs in the mixture was increased. Upon visible irradiation, the toxicity of individual NPs was increased when they coexist as a mixture. It indicates the synergistic action of the mixture, especially when the rutile and anatase NPs were co-exposed in lower quantities. From the synergistic action, the effect of the mixture was slowly transformed into additive action upon an incline in the mixture concentration. In the case of UV-A irradiation, the binary mixture exhibited almost similar toxicity when compared with anatase NPs and higher toxicity with rutile NPs except at their higher concentrations. It implies the additive effect of the mixture under UV-A irradiation except at 1200 μM which depicted an antagonistic effect. These effects have been confirmed with the R_I values computed for the mixture. Thus, the daphnids were highly sensitive to the binary mixture than their individual NPs under both the irradiation conditions. In our previous study, anatase-rutile mixture induced an antagonistic effect on *C. dubia* upon dietary exposure under both irradiation conditions (Iswarya et al. 2018). Similarly, the daphnids exposed to the mixture in the absence of algae (i.e., water-borne) experienced an antagonistic and additive effect upon visible and UV-A irradiation, respectively (Iswarya et al. 2016a). The differences noted in the mortality of daphnids were due to the differential feeding behavior of daphnids which prefers algal cells than the nanoparticles (Dalai et al. 2014). Another rationale behind the changes observed in the mixture toxicity was due to the surface interactions between rutile and anatase NPs in a mixture, which has been evident in the form of NPs aggregation (DLS and TEM data). As a result, the NPs agglomerated algal cells were also available for the ingestion, which in turn induces a significant change in the toxic effect of TiO_2 NPs.

Aggregation profile of TiO_2 NPs in the sterile freshwater

The changes occurring in the size of TiO_2 NPs in the test matrix have been determined over a period of 2 h. TiO_2 NPs either individual or mixture were not stable in the sterile freshwater at the concentrations tested in the study. They have attained micron size within 2 h of irradiation time (Fig. 3). The aggregation profile of different forms of TiO_2 NPs follows a sequential order of rutile > mixture > anatase under both the irradiation conditions analyzed. This result implies that the rutile NPs were highly susceptible to aggregation in the sterile freshwater matrix studied under both visible and UV-A irradiations. TiO_2 NPs undergoes aggregation owing to the interaction with the natural colloids such as dissolved carbon and inorganic ions present in the sterile freshwater (Sillanpää et al. 2011). Furthermore, UV-A exposure induced higher aggregation than the visible irradiation, irrespective of their forms. This effect has been prominent only at the lower concentrations tested. Sun et al. (2014) reported a similar observation, i.e., higher aggregation of P25 NPs upon UV-A irradiation in comparison with non-irradiated NPs suspension. They also elucidated that an incline in the hydroxyl radical's generation, especially the bridging hydroxyls by TiO_2 NPs, was the major factor behind their enhanced aggregation under UV-A irradiation.

Aggregation observed for the binary mixture was also influenced by a typical interfacial interaction between the anatase and rutile NPs in a mixture. It has been evident from the TEM images of the binary mixture that the anatase NPs were encompassed by the rutile NPs (Figs. 4c and 5c) which confirmed their surface interactions when they exist as a binary mixture. EDAX results conveyed the clear information regarding the role of dissolved inorganic ions and carbon in exacerbating the aggregation of individual NPs while they exist as a mixture. Dissolved inorganic ions such as Ca^{2+}, SO_4^{2+}, Cl^-, Na^+, and Mg^{2+}, etc., and organic matter (carbon) present in the freshwater induces a surface complexation with the nanoparticles, which ultimately results in the NPs aggregation (Domingos et al. 2010).

Based on the information obtained from DLS (Fig. 3) and TEM images (Figs. 4 and 5), the probable interaction of TiO_2 NPs (individual as well as a mixture) with the abiotic components of the freshwater has been hypothesized. It has been speculated that the inorganic ions of the freshwater form a thin layer of ions around the NPs to which the natural organic matter (NOM) interacts and binds with them. For individual NPs, this inorganic layer acts as a bridge and provokes the interaction between the NPs and NOM (Chowdhury et al. 2012; Domingos et al. 2010; Metreveli et al. 2016). While in case of the mixture, this inorganic layer and NOM acts as intermediates and induces an electrostatic interaction between anatase and rutile NPs. This NOM binding varies based on the irradiation exposed. It has been presumed that UV-A irradiation infringes the NOM due to the higher ROS generated by the TiO_2 NPs upon photolysis. Thereby, these charged, smaller particles promote the aggregation of NPs in the sterile freshwater upon TiO_2 NPs interaction. In turn, it may lead to sedimentation and affects the bioavailability of NPs to the aquatic organisms present in the system (Aiken et al. 2011; Nur et al. 2015). A schematic representation illustrating the interaction between the anatase and rutile NPs in a mixture has been depicted in Fig. 8.

Oxidative stress markers

Analysis of oxidative stress markers was of prime importance to elucidate the stress impregnated by the nanoparticles on daphnids. It also helps us to determine the defense mechanisms portrayed by the daphnids to cope up with the stress caused by the NPs. Kim et al. (2010) elucidated that the mortality induced by the TiO_2 NPs was ascribed to the oxidative stress generated by the nanoparticles which have been indirectly linked with their antioxidant activities. Hence, some of

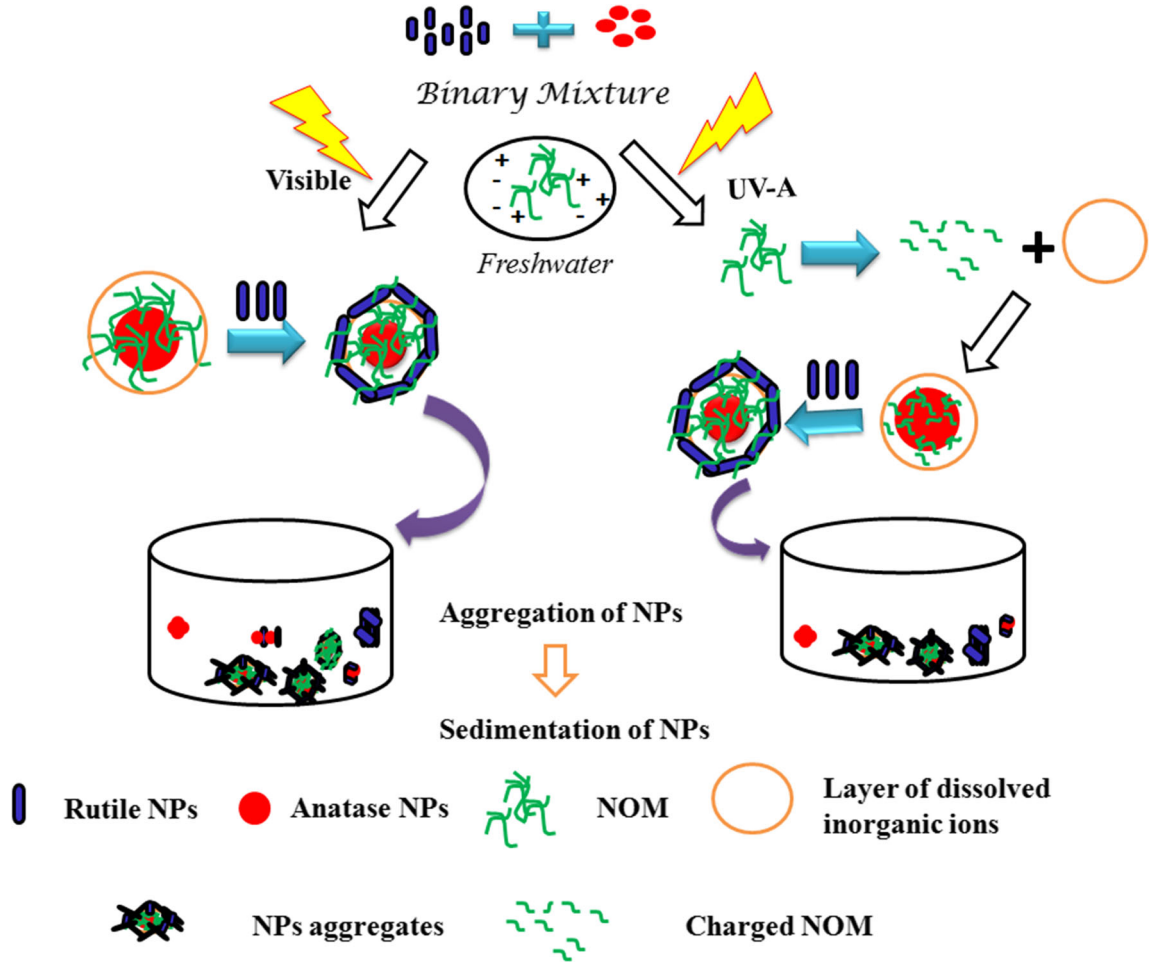

Fig. 8 Schematic diagram representing the transformations and surface interactions between the rutile and anatase NPs in the sterile freshwater when they coexist as a mixture

the important oxidative stress markers such as MDA, catalase, and GSH were evaluated in the current study. MDA is a reactive substance which is highly produced upon the peroxidation of lipids as a consequence of reactive oxygen species (ROS) (Barata et al. 2005). A concentration-dependent incline in the MDA was observed for all the types of NPs tested under UV-A irradiation (Fig. 7a). Even though an increase in MDA was noticed, the MDA levels of anatase NPs were almost similar to the MDA levels of untreated daphnids. In contrast to UV-A, visible irradiation did not induce a concentration-dependent effect on the MDA levels, except the mixture which showed a decrement in the MDA production upon an increase in the concentration (Fig. 6a). Among the different types of TiO_2 tested, rutile NPs depicted the higher amount of MDA production under visible irradiation except at 300 μM, whereas the mixture induced higher quantities of MDA under UV-A irradiation. It depicts the crystalline effect of TiO_2 NPs on the induction of lipid peroxidation. Previous reports illustrated that the excess ROS produced by the nanoparticles interact with the organism's polyunsaturated fatty acids and releases a variety of lipid peroxides including MDA, which eventually activates the antioxidant enzymes like catalase, GST, etc. for detoxification (Bagnyukova et al. 2006; Borgeraas and Hessen 2000; Gao et al. 2017). In addition to ROS, the direct interaction of nanoparticles with the organism also attributes the lipid peroxidation (Federici et al. 2007).

Catalase is an enzymatic antioxidant which catalyzes the H_2O_2 accumulated in the cell and helps in the detoxification mechanism (Halliwell and Gutteridge 2015). Upon exposure to TiO_2 NPs, catalase activity of daphnids was increased significantly than the untreated daphnids (Figs. 6b and 7b). Similar to MDA, an increase observed in the catalase activity was noted to be concentration-dependent under UV-A irradiation and independent upon visible irradiation except the mixture, which showed a decrease in the catalase activity under visible irradiation. Among the different types of TiO_2 tested, mixture depicted higher catalase activity under UV-A. Individually, anatase NPs showed higher catalase activity under UV-A irradiation. However, the catalase activity observed between the particles was not comparable under visible irradiation. The changes observed in the catalase activity were consistent with MDA data, except the anatase NPs under

UV-A. Beyond these differences, catalase activity of daphnids was higher under visible irradiation when compared to UV-A irradiation. Reeves et al. (2008) reported that the by-products of H_2O_2 especially the hydroxyl radicals induced the cytotoxicity on fish cells upon exposure to UV-treated TiO_2 NPs and damaged the major cellular components such as the DNA. Vlahogianni et al. (2007) mentioned that the catalase activity was enhanced to counteract the indirect damages caused by the H_2O_2 accumulation.

Reduced glutathione (GSH) is a non-enzymatic antioxidant molecule which functions as a cofactor for the enzyme glutathione-S-transferase (GST) and protects the integrity of both enzymes and proteins (Mwaanga et al. 2014). In the present study, the amount of reduced glutathione was highly increased in NPs-treated daphnids under both UV-A and visible irradiations (Figs. 6c and 7c). Also, glutathione levels were noted to be independent of concentration under both the irradiations for all the types of TiO_2 NPs tested. A similar concentration-independent effect on GSH levels was observed in mice upon treatment with 30 nm-sized gold NPs (Iswarya et al. 2016b). Contradicting with individual NPs, mixture depicted higher GSH levels under both the irradiation conditions. Among the individual NPs, anatase NPs showed the GSH quantity in higher amounts than the rutile NPs under visible irradiation. In contrast, the GSH levels observed under UV-A irradiation did not show any significant difference among the individual NPs tested in the study. An increase noted in the GSH levels represents a measure taken up by the antioxidant mechanisms to quench the oxidative stress induced. Owing to the large nucleophilic sulfhydryl moieties, GSH was actively involved in the detoxification of H_2O_2 and various other free radicals generated (Knapen et al. 1999). GSH depletion observed at 1200 μM indirectly indicates that the GSH levels were highly utilized by the free radicals generated by the TiO_2 NPs for its neutralization.

Conclusion

The present study explored the toxic effects of various TiO_2 NPs towards *C. dubia* in the presence of algae under distinct irradiation conditions such as visible and UV-A, in context with the freshwater scenario. The outcomes of the study confirm that the availability of algae in the test matrix mitigated the toxic behavior of TiO_2 NPs when exposed individually. The decline in toxicity could have been due to surface modulation of the NPs by interactions with the algal cells or the EPS released by the algae. The binary mixture of rutile and anatase NPs showed enhanced toxicity compared to the individual NPs in the presence of an algal diet, especially under visible irradiation. The surface interaction between the anatase and rutile NPs possibly influenced the toxicity of the mixture. The results from antioxidant enzyme assays supported the mortality data.

Acknowledgements We thank the School of Advanced Sciences (SAS), Vellore Institute of Technology, Vellore, for the TEM facility employed in the study.

Compliance with ethical standards

Conflict of interest The authors declare that they do not have any conflict of interest.

References

Abbott W (1925) A method of computing the effectiveness of an insecticide. J Econ Entomol 18:265–267

Aebi H (1974) Catalase. In: Methods of enzymatic analysis (second edition), volume 2. Elsevier, pp 673-684

Aiken GR, Hsu-Kim H, Ryan JN (2011) Influence of dissolved organic matter on the environmental fate of metals, nanoparticles, and colloids. ACS Publications

Allen HJ, Impellitteri CA, Macke DA, Heckman JL, Poynton HC, Lazorchak JM, Govindaswamy S, Roose DL, Nadagouda MN (2010) Effects from filtration, capping agents, and presence/absence of food on the toxicity of silver nanoparticles to *Daphnia magna*. Environ Toxicol Chem 29:2742–2750

Bagnyukova TV, Chahrak OI, Lushchak VI (2006) Coordinated response of goldfish antioxidant defenses to environmental stress. Aquat Toxicol 78:325–331

Bai Y, Mora-Sero I, De Angelis F, Bisquert J, Wang P (2014) Titanium dioxide nanomaterials for photovoltaic applications. Chem Rev 114: 10095–10130

Barata C, Varo I, Navarro JC, Arun S, Porte C (2005) Antioxidant enzyme activities and lipid peroxidation in the freshwater cladoceran *Daphnia magna* exposed to redox cycling compounds. Comp Biochem Physiol Part C: Toxicol Pharmacol 140:175–186

Borgeraas J, Hessen DO (2000) UV-B induced mortality and antioxidant enzyme activities in *Daphnia magna* at different oxygen concentrations and temperatures. J Plankton Res 22:1167–1183

Botta C et al (2011) TiO_2-based nanoparticles released in water from commercialized sunscreens in a life-cycle perspective. Struct Quant Environ Poll 159:1543–1550. https://doi.org/10.1016/j.envpol.2011.03.003

Bottero J-Y, Wiesner MR (2010) Considerations in evaluating the physicochemical properties and transformations of inorganic nanoparticles in water. Nanomedicine 5:1009–1014

Buege JA, Aust SD (1978) [30] Microsomal lipid peroxidation. In: Methods in enzymology, vol 52. Elsevier, pp 302-310

Chesworth J, Donkin M, Brown M (2004) The interactive effects of the antifouling herbicides Irgarol 1051 and Diuron on the seagrass *Zostera marina* (L.). Aquat Toxicol 66:293–305

Chowdhury I, Cwiertny DM, Walker SL (2012) Combined factors influencing the aggregation and deposition of nano-TiO_2 in the presence of humic acid and bacteria. Environ Sci Technol 46:6968–6976

Clemente Z, Castro V, Jonsson C, Fraceto L (2014) Minimal levels of ultraviolet light enhance the toxicity of TiO_2 nanoparticles to two representative organisms of aquatic systems. J Nanopart Res 16: 2559

Conine AL, Frost PC (2017) Variable toxicity of silver nanoparticles to *Daphnia magna*: effects of algal particles and animal nutrition. Ecotoxicology 26:118–126

Costa PCDO (2015) Effects of mixture of nanoparticles under different salinity in the clams *Ruditapes philippinarum* and *Ruditapes decussatus*

Dalai S, Iswarya V, Bhuvaneshwari M, Pakrashi S, Chandrasekaran N, Mukherjee A (2014) Different modes of TiO_2 uptake by *Ceriodaphnia dubia*: relevance to toxicity and bioaccumulation. Aquat Toxicol 152:139–146

Dalai S, Pakrashi S, Nirmala MJ, Chaudhri A, Chandrasekaran N, Mandal A, Mukherjee A (2013) Cytotoxicity of TiO_2 nanoparticles and their detoxification in a freshwater system. Aquat Toxicol 138: 1–11

Das P, Xenopoulos MA, Metcalfe CD (2013) Toxicity of silver and titanium dioxide nanoparticle suspensions to the aquatic invertebrate, *Daphnia magna*. Bull Environ Contam Toxicol 91:76–82

Domingos RF, Peyrot C, Wilkinson KJ (2010) Aggregation of titanium dioxide nanoparticles: role of calcium and phosphate. Environ Chem 7:61–66

Fan J, Li Z, Zhou W, Miao Y, Zhang Y, Hu J, Shao G (2014) Dye-sensitized solar cells based on TiO_2 nanoparticles/nanobelts double-layered film with improved photovoltaic performance. Appl Surf Sci 319:75–82

Federici G, Shaw BJ, Handy RD (2007) Toxicity of titanium dioxide nanoparticles to rainbow trout (*Oncorhynchus mykiss*): gill injury, oxidative stress, and other physiological effects. Aquat Toxicol 84: 415–430

Gao C, Zhang X, Xu N, Tang X Toxic effects of combined effects of anthracene and UV radiation on *Brachionus plicatilis*. In: IOP Conference Series: earth and environmental science, 2017. vol 1. IOP Publishing, p 012121

Gondikas AP, Kammer F, Reed RB, Wagner S, Ranville JF, Hofmann T (2014) Release of TiO_2 nanoparticles from sunscreens into surface waters: a one-year survey at the old Danube recreational Lake. Environ Sci Technol 48:5415–5422

Gottschalk F, Lassen C, Kjoelholt J, Christensen F, Nowack B (2015) Modeling flows and concentrations of nine engineered nanomaterials in the Danish environment. Int J Environ Res Public Health 12:5581–5602

Halliwell B, Gutteridge JM (2015) Free radicals in biology and medicine. Oxford University Press, USA

Harifi T, Montazer M (2017) Application of nanotechnology in sports clothing and flooring for enhanced sport activities, performance, efficiency and comfort: a review. J Ind Text 46:1147–1169

Hegde K, Brar SK, Verma M, Surampalli RY (2016) Current understandings of toxicity, risks and regulations of engineered nanoparticles with respect to environmental microorganisms. Nanotechnol Environ Eng 1:5. https://doi.org/10.1007/s41204-016-0005-4

Huang Y-W, Wu C-h, Aronstam RS (2010) Toxicity of transition metal oxide nanoparticles: recent insights from in vitro studies. Materials 3:4842–4859

Hund-Rinke K, Simon M (2006) Ecotoxic effect of photocatalytic active nanoparticles (TiO_2) on algae and daphnids. Environ Sci Pollut Res Int 13:225–232. https://doi.org/10.1065/espr2006.06

Iswarya V, Bhuvaneshwari M, Alex SA, Iyer S, Chaudhuri G, Chandrasekaran PT, Bhalerao GM, Chakravarty S, Raichur AM, Chandrasekaran N, Mukherjee A (2015) Combined toxicity of two crystalline phases (anatase and rutile) of Titania nanoparticles towards freshwater microalgae: *Chlorella* sp. Aquat Toxicol 161: 154–169. https://doi.org/10.1016/j.aquatox.2015.02.006

Iswarya V, Manivannan J, de A, Paul S, Roy R, Johnson JB, Kundu R, Chandrasekaran N, Mukherjee A, Mukherjee A (2016b) Surface capping and size-dependent toxicity of gold nanoparticles on different trophic levels. Environ Sci Pollut Res 23:4844–4858

Iswarya V, Bhuvaneshwari M, Chandrasekaran N, Mukherjee A (2016a) Individual and binary toxicity of anatase and rutile nanoparticles towards *Ceriodaphnia dubia*. Aquat Toxicol 178:209–221. https://doi.org/10.1016/j.aquatox.2016.08.007

Iswarya V, Bhuvaneshwari M, Chandrasekaran N, Mukherjee A (2018) Trophic transfer potential of two different crystalline phases of TiO_2 NPs from *Chlorella* sp. to *Ceriodaphnia dubia*. Aquat Toxicol 197: 89–97

Jacobasch C, Völker C, Giebner S, Völker J, Alsenz H, Potouridis T, Heidenreich H, Kayser G, Oehlmann J, Oetken M (2014) Long-term effects of nanoscaled titanium dioxide on the cladoceran *Daphnia magna* over six generations. Environ Pollut 186:180–186

Jiang LC, Zhang WD (2009) Electrodeposition of TiO_2 nanoparticles on multiwalled carbon nanotube arrays for hydrogen peroxide sensing. Electroanalysis 21:988–993

Kathawala MH, Ng KW, Loo SCJ (2015) TiO_2 nanoparticles alleviate toxicity by reducing free Zn^{2+} ion in human primary epidermal keratinocytes exposed to ZnO nanoparticles. J Nanopart Res 17:263

Keller AA, McFerran S, Lazareva A, Suh S (2013) Global life cycle releases of engineered nanomaterials. J Nanopart Res 15:1692

Kim KT, Klaine SJ, Cho J, Kim S-H, Kim SD (2010) Oxidative stress responses of *Daphnia magna* exposed to TiO_2 nanoparticles according to size fraction. Sci Total Environ 408:2268–2272

Knapen MF, Zusterzeel PL, Peters WH, Steegers EA (1999) Glutathione and glutathione-related enzymes in reproduction: a review. Eur J Obstet Gynecol Reprod Biol 82:171–184

Ko K-S, Koh D-C, Kong IC (2017) Evaluation of the effects of nanoparticle mixtures on Brassica seed germination and bacterial bioluminescence activity based on the theory of probability. Nanomaterials 7:344

Ko K-S, Koh D-C, Kong IC (2018) Toxicity evaluation of individual and mixtures of nanoparticles based on algal chlorophyll content and cell count. Materials 11:121

Lampert W (1987) Laboratory studies on zooplankton-cyanobacteria interactions New Zealand. Aust J Mar Freshwat Res 21:483–490

Li S, Ma H, Wallis LK, Etterson MA, Riley B, Hoff DJ, Diamond SA (2016) Impact of natural organic matter on particle behavior and phototoxicity of titanium dioxide nanoparticles. Sci Total Environ 542:324–333. https://doi.org/10.1016/j.scitotenv.2015.09.141

Lu G, Yang H, Xia J, Zong Y, Liu J (2017a) Toxicity of Cu and Cr nanoparticles to *Daphnia magna* water. Air Soil Pollut 228:18

Lu H, Fan W, Dong H, Liu L (2017b) Dependence of the irradiation conditions and crystalline phases of TiO_2 nanoparticles on their toxicity to *Daphnia magna*. Environ Sci Nano 4:406–414

McWilliams A, (2014) global markets for nanocomposites, nanoparticles, nanoclays, and nanotubes. BBC Research

Metreveli G et al (2016) Impact of chemical composition of ecotoxicological test media on the stability and aggregation status of silver nanoparticles. Environ Sci Nano 3:418–433

Mueller NC, Nowack B (2008) Exposure modeling of engineered nanoparticles in the environment. Environ Sci Technol 42:4447–4453

Mwaanga P, Carraway ER, van den Hurk P (2014) The induction of biochemical changes in *Daphnia magna* by CuO and ZnO nanoparticles. Aquat Toxicol 150:201–209

Nur Y, Lead J, Baalousha M (2015) Evaluation of charge and agglomeration behavior of TiO_2 nanoparticles in ecotoxicological media. Sci Total Environ 535:45–53

OECD (2004) Test no. 202: Daphnia sp. acute immobilisation test. OECD Publishing

Ou G, Li Z, Li D, Cheng L, Liu Z, Wu H (2016) Photothermal therapy by using titanium oxide nanoparticles. Nano Res 9:1236–1243

Reeves JF, Davies SJ, Dodd NJ, Jha AN (2008) Hydroxyl radicals (OH) are associated with titanium dioxide (TiO_2) nanoparticle-induced cytotoxicity and oxidative DNA damage in fish cells mutation research/fundamental and molecular mechanisms of mutagenesis. Mutat Res 640:113–122

Sedlak J, Lindsay RH (1968) Estimation of total, protein-bound, and nonprotein sulfhydryl groups in tissue with Ellman's reagent. Anal Biochem 25:192–205

Sendra M, Moreno-Garrido I, Yeste M, Gatica J, Blasco J (2017) Toxicity of TiO_2, in nanoparticle or bulk form to freshwater and marine microalgae under visible light and UV-A radiation. Environ Pollut 227:39–48

Shandilya N, Le Bihan O, Bressot C, Morgeneyer M (2015) Emission of titanium dioxide nanoparticles from building materials to the environment by wear and weather. Environ Sci Technol 49:2163–2170

Sillanpää M, Paunu T-M, Sainio P Aggregation and deposition of engineered TiO_2 nanoparticles in natural fresh and brackish waters. In: Journal of Physics: Conference Series, 2011. vol 1. IOP Publishing, p 012018

Sun J, Guo L-H, Zhang H, Zhao L (2014) UV irradiation induced transformation of TiO_2 nanoparticles in water: aggregation and photoreactivity. Environ Sci Technol 48:11962–11968

Tatarazako N, Oda S (2007) The water flea *Daphnia magna* (Crustacea, Cladocera) as a test species for screening and evaluation of chemicals with endocrine disrupting effects on crustaceans. Ecotoxicology 16:197–203

Vance ME, Kuiken T, Vejerano EP, McGinnis SP, Hochella MF Jr, Rejeski D, Hull MS (2015) Nanotechnology in the real world: redeveloping the nanomaterial consumer products inventory. Beilstein J Nanotechnol 6:1769–1780

Vlahogianni T, Dassenakis M, Scoullos MJ, Valavanidis A (2007) Integrated use of biomarkers (superoxide dismutase, catalase and lipid peroxidation) in mussels *Mytilus galloprovincialis* for assessing heavy metals' pollution in coastal areas from the Saronikos Gulf of Greece. Mar Pollut Bull 54:1361–1371

Wang A-n, Teng Y, Hu X-f, Wu L-h, Y-j H, Luo Y-m, Christie P (2016) Diphenylarsinic acid contaminated soil remediation by titanium dioxide (P25) photocatalysis: degradation pathway, optimization of operating parameters and effects of soil properties. Sci Total Environ 541:348–355

Wang Z et al (2017) Trophic transfer of TiO_2 nanoparticles from marine microalga (*Nitzschia closterium*) to scallop (*Chlamys farreri*) and related toxicity. Environ Sci: Nano 4:415–424

Windler L, Lorenz C, von Goetz N, Hungerbuhler K, Amberg M, Heuberger M, Nowack B (2012) Release of titanium dioxide from textiles during washing. Environ Sci Technol 46:8181–8188

Wormington AM, Coral J, Alloy MM, Delmarè CL, Mansfield CM, Klaine SJ, Bisesi JH, Roberts AP (2017) Effect of natural organic matter on the photo-induced toxicity of titanium dioxide nanoparticles. Environ Toxicol Chem 36:1661–1666

Yang Y, Doudrick K, Bi X, Hristovski K, Herckes P, Westerhoff P, Kaegi R (2014) Characterization of food-grade titanium dioxide: the presence of nanosized particles. Environ Sci Technol 48:6391–6400

Ye N, Wang Z, Fang H, Wang S, Zhang F (2017) Combined ecotoxicity of binary zinc oxide and copper oxide nanoparticles to *Scenedesmus obliquus*. J Environ Sci Health A 52:555–560

Ye N, Wang Z, Wang S, Peijnenburg WJ (2018) Toxicity of mixtures of zinc oxide and graphene oxide nanoparticles to aquatic organisms of different trophic level: particles outperform dissolved ions. Nanotoxicology 12:1–16

Yu H, Pan J, Bai Y, Zong X, Li X, Wang L (2013) Hydrothermal synthesis of a crystalline rutile TiO_2 nanorod based network for efficient dye-sensitized solar cells. Chem-A Eur J 19:13569–13574

Zahra Z, Waseem N, Zahra R, Lee H, Badshah MA, Mehmood A, Choi HK, Arshad M (2017) Growth and metabolic responses of rice (*Oryza sativa* L.) cultivated in phosphorus-deficient soil amended with TiO_2 nanoparticles. J Agric Food Chem 65:5598–5606

Zou X, Shi J, Zhang H (2014) Coexistence of silver and titanium dioxide nanoparticles: enhancing or reducing environmental risks? Aquat Toxicol 154:168–175